Proceedings of the XII International Symposium on Dynamic Problems of Mechanics (DINAME 2007),
Varoto, P. S. and Trindade, M. A. (Editors), ABCM, Ilhabela, SP, Brazil, February 26 - March 2, 2007

Axisymmetric Finite Element Model Representation of Composite Tubes

Almeida.C. A.[1] and Guimarães, G. P.[2]

[1] Pontifícia Universidade Católica do Rio de Janeiro, PUC-Rio , R. Marquês de S. Vicente, 225, Gávea, Rio de Janeiro, RJ 22453-900

[2] CTEx - Centro Tecnológico do Exército, Av. das Américas 28705, Guaratiba, Rio de Janeiro, RJ 23020-470

Abstract: This work deals with modeling, implementation and testing of an axisymmetric finite element formulation that represents the mechanical behavior of fibrous laminated composite tubes under internal/external pressure and other general symmetrical loadings. The model discretization is attained to the tube generating rectangular section by using a quadrilateral four node element mesh, with three displacement degrees-of-freedom per node represented in a cylindrical coordinate system attached to tube axis. Composite laminated layers are assumed perfectly bonded together, assuring material continuity between the layers on the displacement fields. Orthotropic and/or transverse isotropic constitutive material laws have been implemented, allowing for displacement, strain and stress numerical solutions. In the element model validation, results from the present finite element model are compared with those from analytical solutions available in the literature as well as from the use of layered solid element model available in a commercial finite element program. Two sample examples of a two-layer composite [-45°/+45°] material were considered for model testing compared to theoretical and numerical solutions. Good numerical convergence in the solutions presented, which represent the main characteristics for this class of problems, is noted.

Keywords: composite materials, laminate structure, finite element model, axisymmetric formulation

NOMENCLATURE

h_i= Lagrange interpolation function, referred to node i
r,s = element local coordinates ($-1 \le r,s \le +1$)
r_i = radial coordinate, at node i
u_i = axial displacement, at node i
v_i = circumferential displacement, at node i
w_i = radial displacement, at node i
x_i = axial coordinate, at node i
B(r,s) = element strain-displacement matrix
C = constitutive matrix, referred to global coordinate X-θ-R system
$\overline{C}$ = constitutive matrix, referred to local coordinate 1-2-3 system
E = modulus of elasticity
G = shear modulus
J = element Jacobian matrix
K = element stiffness matrix
M_1 = stress transformation matrix, from local to the global coordinate system
M_2 = strain transformation matrix, from local to the global coordinate system
R = global radial coordinate
U = global axial displacement
V = global circumferential displacement
W = global radial displacement
X = global axial coordinate

Greek Symbols

ε = linear strain component
$\boldsymbol{\varepsilon}$ = strain component vector, in global coordinate X-θ-R system
$\overline{\boldsymbol{\varepsilon}}$ = strain component vector, in local coordinate 1-2-3 system
$\boldsymbol{\sigma}$ = stress component vector, in global coordinate X-θ-R system
$\overline{\boldsymbol{\sigma}}$ = stress component vector, in local coordinate 1-2-3 system
γ = shear strain component
υ = Poisson's ratio

Subscripts

ii,jj,ij = relative to material local axis
xx, θθ, RR, etc = relative to plane and directions of strains and stresses

INTRODUCTION

Circular cylindrical tubes are widely used in engineering practice, especially in chemical, offshore and infrastructure applications. They are also present in living organisms, with a diversity of applications in carrying fluids such in blood vessels or elephant trunks. Today, fibrous composites are fabricated to meet piping specifications which can be fabricated by various methods such filament winding and pultrusion. Material selection, fiber orientations, and layer thickness are some of the engineering parameters for an optimized piping design. As examples, tubular configuration structures in living organisms are invariably laminated to meet their needs for a specific use, while piping hybrid composite structures are employed in special applications such oil drilling operations and in aerospace industries. These piping structures have as major advantage the combination of low weight with high mechanical strength and are obtained by layer superposition of composite materials, forming a laminate. These combined laminae results in an orthotropic structure with some very useful mechanical properties, improving axial, torsion and global bending stiffness throughout axial-torsion kinematics couplings.

Analytical solutions for composite tubes are only available for the linear elastic material behavior, under special types of loading and boundary conditions. They are based, for example, upon the works of Lekhnitskii(1950), Scherrer(1967), Pagano(1971), Reissner and Tsai(1974), Wilson and Orgill(1986), assuming perfectly bounded layers. In practice these types of structures are subjected to internal/external pressure, longitudinal traction or compression and torsion. However, the solutions reported in these works refer to a long pipe with a number of layers and material constitutive parameters, under internal pressure only. Displacement, strains and stress fields along the thickness of the pipe are the obtained solutions provided. Orthotropic and transverse isotropic constitutive relations are used in the material characterization and displacement continuity conditions are granted throughout the pipe layers.

In this paper a finite element formulation is presented towards the representation of composite cylindrical tubes. It employs a four-node isoparametric finite element formulation, with three displacements per node defined in the axial, circumferential and radial directions of the cylinder. Material isotropy, transverse isotropy and orthotropy are allowed, under static analysis, considering internal/external pressure, axial and torsion loadings, all varying along the pipe length. The formulation equations are set based in linear theory of elasticity relations, under the axisymmetry geometric condition.

In the next section, the formulation is presented so that the element is applicable to the modeling of composite pipes. The appropriate discretized equations for constitutive, geometric compatibility and equilibrium conditions, imposed to each layer, are derived. The element formulation has been implemented and some sample analysis results are presented and compared with numerical solutions obtained from other commercial finite element software.

Element Kinematics and F E Formulation

Considering a circular tube composed by anisotropic layers, the finite element representation consists on discretizing the displacements in each layer using the appropriate cylindrical coordinate referred to its axis of symmetry. The problem axisymmetry - geometry and loading - results in spatial displacements varying in radial an axial direction, only. Thus, two-dimension elements are used in the numerical representation of the cylinder, representing its rectangular generatrix section. The four-node element, with Lagrange interpolation functions, is employed for geometry and kinematics representation, as shown in Fig. 1. Thus, geometric coordinates are defined as

$$X(r,s) = \sum_{i=1}^{4} h_i(r,s)\, x_i \ , \ R(r,s) = \sum_{i=1}^{4} h_i(r,s)\ r_i \qquad (1)$$

and for the displacements we have

$$U(r,s) = \sum_{i=1}^{4} h_i(r,s)\, u_i \quad , \quad V(r,s) = \sum_{i=1}^{4} h_i(r,s)\, v_i \quad \text{and} \quad W(r,s) = \sum_{i=1}^{4} h_i(r,s)\, w_i \ . \qquad (2)$$

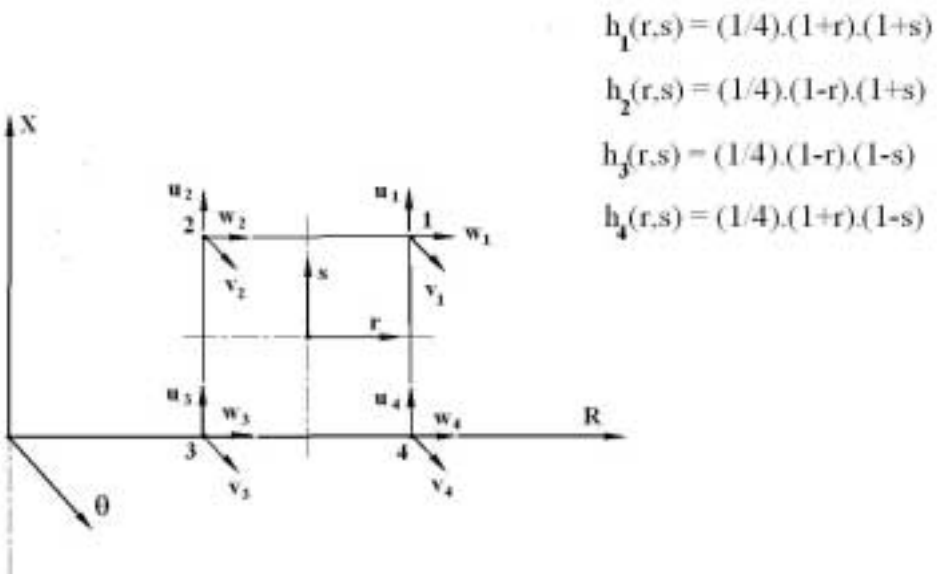

Figure 1 – Element Nodal Displacements and Interpolation Functions Used

Combining these two sets of equations the displacement fields can be written with respect to geometric global coordinates X and R, such that U(X,R), V(X,R) and W(X,R) are stated. From these, the element strains are evaluated in

the element cylindrical coordinate system, referrer to the global X-θ-R axis, as shown in Fung (1965). Thus, the following strain components are obtained

$$\varepsilon_{XX} = \partial U/\partial X\,, \quad \varepsilon_{\theta\theta} = W/R\,, \quad \varepsilon_{RR} = \partial W/\partial R \quad \text{and}$$
$$\gamma_{X\theta} = \partial V/\partial X \quad \gamma_{XR} = \partial U/\partial R + \partial W/\partial X \quad \gamma_{\Theta r} = \partial V/\partial R - V/R \tag{3}$$

which, after discretization eqs. (1) and (2) being considered, result in a twelve degree-of-freedom finite element, with the following displacement vector associated to each element ,

$$\mathbf{U^T} = [\, u_1 \;\; v_1 \;\; w_1 \;\; u_2 \;\; v_2 \;\; w_2 \;\; u_3 \;\; v_3 \;\; w_3 \;\; u_4 \;\; v_4 \;\; w_4 \,]\,. \tag{4}$$

In eqs. (3) nodal displacement differentiation is taken using

$$\boldsymbol{\partial/\partial X} = \mathbf{J^{-1}}\;\boldsymbol{\partial/\partial r}\,, \tag{5}$$

where

$$\mathbf{J} = \begin{bmatrix} \partial X/\partial r & \partial R/\partial r \\ \partial X/\partial s & \partial R/\partial s \end{bmatrix} \tag{6}$$

is the element Jacobian matrix, obtained from coordinate definitions set in eq. (1), and

$$\boldsymbol{\partial/\partial X}^{\mathrm{T}} = [\, \partial/\partial X \;\; \partial/\partial R \,] \quad \text{and} \quad \boldsymbol{\partial/\partial r}^{\mathrm{T}} = [\, \partial/\partial r \;\; \partial/\partial s \,]\,. \tag{7}$$

Thus, combining equations (3) to (7), the element strain vector relates to nodal point displacements, in matrix form, as

$$\boldsymbol{\varepsilon} = \mathbf{B}(r,s)\,\mathbf{U} \tag{8}$$

with the following matrix elements definitions, for i= 0,1, 2 and 3,

$$\begin{aligned}
B_{1,1+3i}(r,s) &= J^{-1}_{11}\, h_{i,r} + J^{-1}_{12}\, h_{i,s}\,,\\
B_{2,3+3i}(r,s) &= h_i/R\,,\\
B_{3,3+3i}(r,s) &= J^{-1}_{21}\, h_{i,r} + J^{-1}_{22}\, h_{i,s}\,,\\
B_{4,2+3i}(r,s) &= J^{-1}_{11}\, h_{i,r} + J^{-1}_{12}\, h_{i,s}\,,\\
B_{5,1+3i}(r,s) &= J^{-1}_{21}\, h_{i,r} + J^{-1}_{22}\, h_{i,s}\,,\\
B_{5,3+3i}(r,s) &= J^{-1}_{11}\, h_{i,r} + J^{-1}_{12}\, h_{i,s}\,,\\
B_{6,2+3i}(r,s) &= J^{-1}_{21}\, h_{i,r} + J^{-1}_{22}\, h_{i,s} - h_i/R
\end{aligned} \tag{9}$$

and all others equal to zero.

Model constants for the composite material are generally defined using fiber directions as coordinate axis of reference, in which no couplings between normal and shear stress components occur. Setting these as 1-2-3 directions, shown in Fig. 2, the element constitutive relation, for orthotropic materials, becomes

$$\overline{\sigma} = \overline{C}\;\overline{\varepsilon} \tag{10}$$

with,

$$\overline{C} = \begin{bmatrix} 1/E_{11} & -\upsilon_{21}/E_{22} & -\upsilon_{31}/E_{33} & 0 & 0 & 0 \\ -\upsilon_{12}/E_{11} & 1/E_{22} & -\upsilon_{32}/E_{33} & 0 & 0 & 0 \\ -\upsilon_{13}/E_{11} & -\upsilon_{23}/E_{22} & 1/E_{33} & 0 & 0 & 0 \\ 0o & 0 & 0 & 1/G_{12} & 0 & 0 \\ 0 & 0 & 0 & 0 & 1/G_{13} & 0 \\ 0 & 0 & 0 & 0 & 0 & 1/G_{23} \end{bmatrix}\,. \tag{11}$$

In eq.(11) E_{ii}'s are the Young's modulus in each local direction, G_{ij}'s and υ_{ij}'s – for i≠j – are the material shear modulus and Poisson's ratio, respectively, while

$$\upsilon_{ij} = (E_{ii}/E_{jj})\,\upsilon_{ji}\,, \tag{12}$$

as required from symmetry. Also, in this work, direction-1 has been set as the fibers direction in the composite and the material considered as transversally isotropic, what gives

$$E_{22} = E_{33},\ \upsilon_{12} = \upsilon_{13},\ G_{12} = G_{13} \text{ and } G_{23} = E_{22}/2(1+\upsilon_{23}). \tag{13}$$

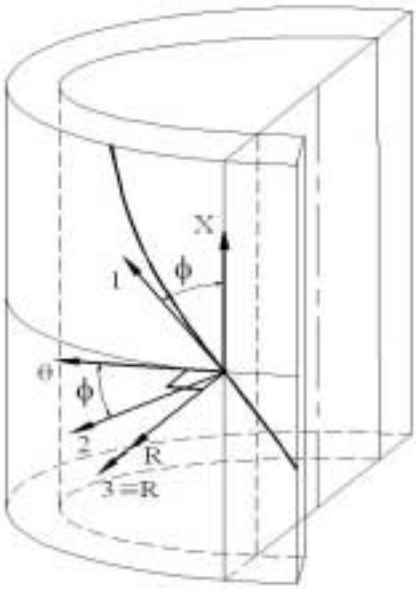

Figure 2 – Local Coordinates for The Composite Material Fibers

Thus, the number of required parameters for the constitutive relation matrix $\overline{C}$ reduces to the following five constants: $E_{11},\ E_{22}, G_{12}, \upsilon_{12}, \upsilon_{13}$. Using the appropriate coordinate transformations to the global coordinate system X-θ-R , stress and strain vectors are defined, respectively, as

$$\overline{\sigma} = M_1\ \sigma \tag{14}$$

$$\text{and } \overline{\varepsilon} = M_2\ \varepsilon \tag{15}$$

with

$$M_1 = \begin{bmatrix} m^2 & n^2 & 0 & 2mn & 0 & 0 \\ n^2 & m^2 & 0 & -2mn & 0 & 0 \\ 0 & 0 & 1 & 0 & 0 & 0 \\ -mn & mn & 0 & (m^2-n^2) & 0 & 0 \\ 0 & 0 & 0 & 0 & m & n \\ 0 & 0 & 0 & 0 & -n & m \end{bmatrix} \text{ and } M_2 = \begin{bmatrix} m^2 & n^2 & 0 & mn & 0 & 0 \\ n^2 & m^2 & 0 & -mn & 0 & 0 \\ 0 & 0 & 1 & 0 & 0 & 0 \\ -2mn & 2mn & 0 & (m^2-n^2) & 0 & 0 \\ 0 & 0 & 0 & 0 & m & n \\ 0 & 0 & 0 & 0 & -n & m \end{bmatrix}. \tag{16}$$

where m ≡ cos φ and n ≡ sin φ definitions are employed, as shown in Lardner and Archer(1994).

Substituting eqs. (14) and (15) into eq. (10), the element constitutive relation, referred to the global coordinate system, results in

$$\sigma = C\ \varepsilon \tag{17}$$

with $C = M_1^{-1}\ \overline{C}\ M_2$.

Using the principle of virtual work (or principle of minimum total potential energy) to derive the equilibrium equations for the linear response of the element we obtain, as in Bathe(1996),

$$\mathbf{K\ U = R} \tag{18}$$

where **K** is the stiffness matrix of the finite element corresponding to the element nodal point degrees-of-freedom listed in **U**,

$$\mathbf{K} = \int_V \mathbf{B}^{\mathrm{T}}\, C\, \mathbf{B}\ \mathrm{d}V \tag{19}$$

and **R** is the effective nodal point load vector.

Sample Analyses

The element formulation has been implemented and the numerical solutions of the following two analyses indicate its applicability and effectiveness. In both examples a two-layer composite cylinder under internal pressure is considered having [+45°/-45°] winding orientations, with respect to the longitudinal axis of the cylinder. The two analyses differ on the boundary conditions employed, for which this type of structure arrangement is very sensitive, as shown in the examples. In both cases a 30in. internal diameter, 6in. thick and 1in. long cylinder was considered, under a 10 psi. internal pressure. The cylinder composite – transversally isotropic – material used has the following characteristic constants: $E_{11} = 19{,}2\text{x}10^6$ psi, $E_{22} = 1{,}56\text{x}10^6$ psi, $G_{12} = 0{,}82\text{x}10^6$ psi, $\upsilon_{12} = 0{,}24$ and $\upsilon_{23} = 0{,}49$.

Case 1 – Comparison to Analytical Solutions

In this case the numerical analysis results are compared with the analytical solutions obtained by Herakovich (1998). A model of eight equally spaced elements, in the radial direction, was used, according to the convergence study presented by Guimarães(2006). For these comparisons the tube boundary conditions were set as follows: a) axial and circumferential displacements at bottom nodes are fixed and, b) at the upper nodes, axial displacements are equally imposed while the circumferential displacements are set proportional to the radial coordinate of each node (as in a tor-

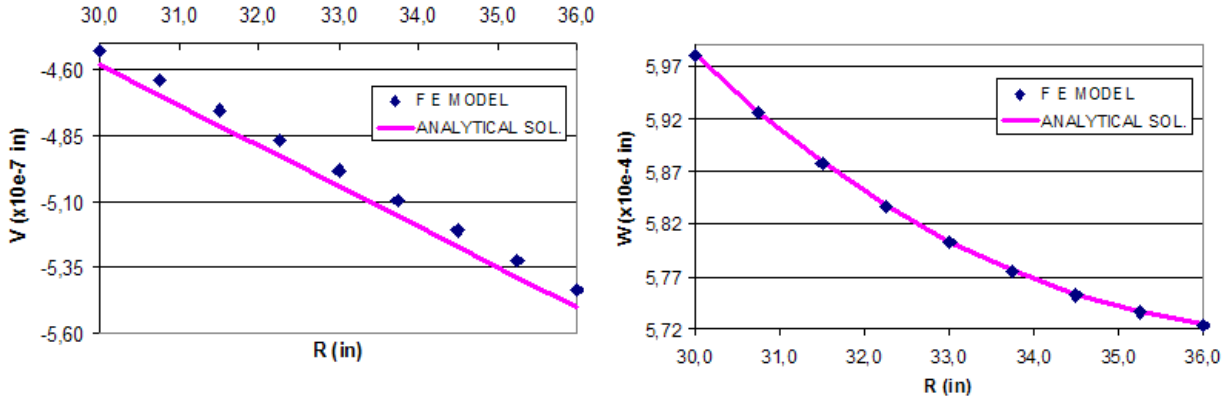

Figure 3 – Circumferential and Radial Displacements at the Model Upper Face Nodes, for Case 1 Analysis

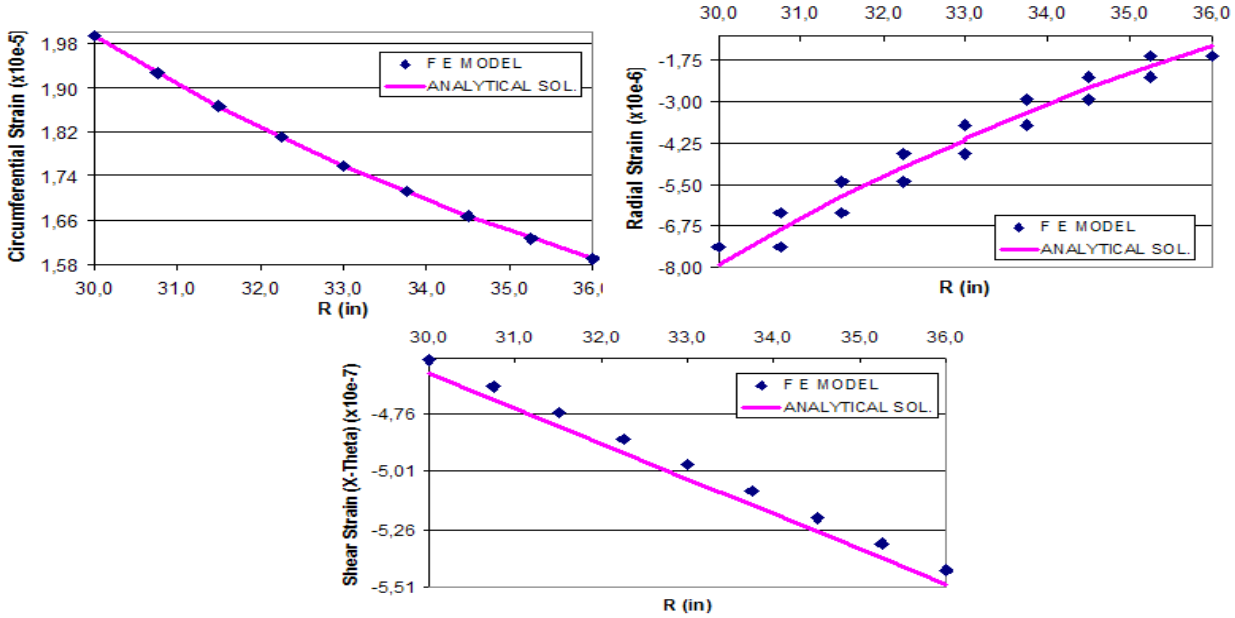

Figure 4 – Strain Component at the Model Upper Face Nodes, for Case 1 Analysis

sion mode). These boundary conditions were set such that they reproduce the analytical solution sough.

The finite element results are all presented at the element nodal points. For the axial displacement at the model upper nodes they resulted in an error less than 0,004%, with respect to the analytical solution. Circumferential and radial displacement comparisons, along the radial coordinate, are shown in Figs. 3. A very good agreement for the radial displacements-W is observed, as they represent the largest displacement values in the model. Strain results are

compared in Fig. 4. Circumferential strain distributions ($\varepsilon_{\theta\theta}$) agreed quite well with the analytical solutions, while radial (ε_{RR}) and shear ($\gamma_{X\theta}$) strains present some differences. These are mainly due to the order of the interpolation functions employed in the formulation, what resulted in constant numerical values for the radial strain component, within each element, and a discontinuity at the nodes. Moreover, these two numerical results are, at least, one order of magnitude smaller than the largest circumferential strains $\varepsilon_{\theta\theta}$, validating the model discretization used, as shown in the displacement solutions in Fig.3. Stress component distributions are presented in Fig. 5. A good agreement in the results is obtained, except for the radial stresses which are very much affected by the approximations employed in the model for the radial strain distribution. As in the previous comparison, these stress components are, at least, one order of magnitude low than the circumferential and the shear stress values. It is noticeable, in the graphs, sharp stress distribution discontinuities at the layer changing node, in the tube radial direction. The largest stress value jump occurs in the shear (X-Theta) distribution, what is the main cause for degradation of the composite materials, such delamination failures, as reported in the literature by Herakovick (1979 and 1989).

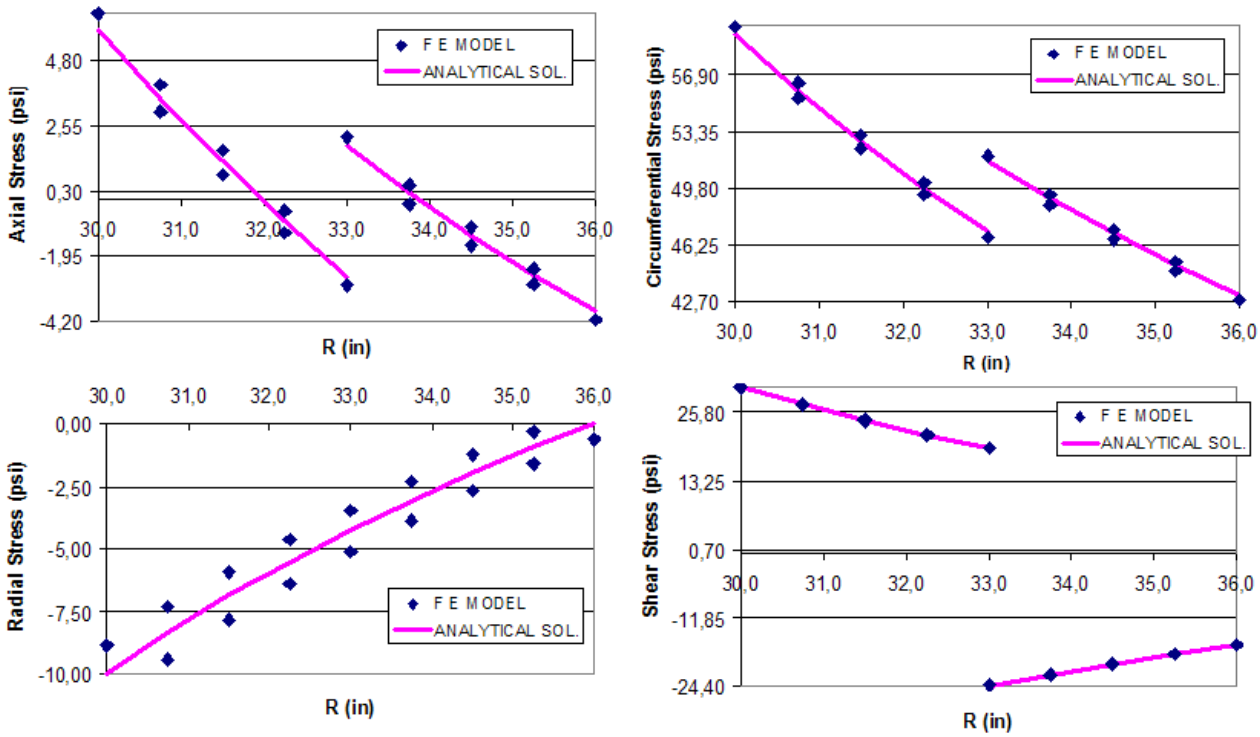

Figure 5 – Stress Components at the Model Upper Face Nodes, for Case 1 Analysis

Case 2 – Comparison to Other Numerical Solutions

A more realistic numerical comparison, with the results furnished by the commercial finite element code ANSYS, is set in this analysis. The finite element model furnished by this study employed twelve equally spaced elements – in the radial direction - with the boundary conditions set, only at the bottom nodes, as fixed displacements in axial and circumferential directions. ANSYS finite element program model was used for comparison: the same number of elements in the radial direction but a total of 2400 brick – eight node elements – to represent the entire ring structure. Only one layer of elements was used in the axial direction. The use of such model was motivated by the need of an evaluation of the problem as defined by an axisymmetric structure, what was confirmed by the three nodal displacement results provided by ANSYS analysis, which varied in axial and radial directions only.

Figure 6 presents solution comparisons for axial, circumferential and radial displacements at the model upper face nodes, along the radial direction. It can be noticed a good agreement between the numerical results – with an error not larger than 2% - and, as in the previous analysis, the largest absolute value for the displacements occurred in the radial direction. However, as per the circumferential displacements-V no similarity to classical torsion kinematics is observed, as stated in the analytical model discussed in Case 1 analysis.

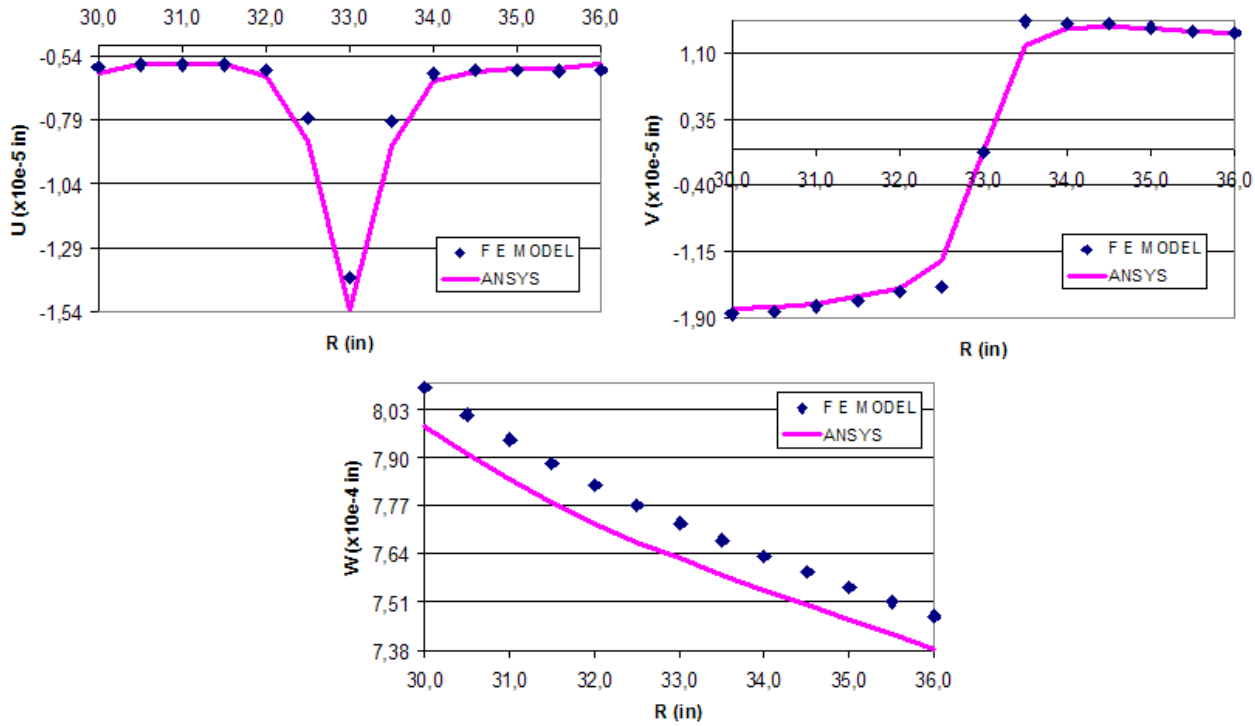

Figure 6 – Displacements at the Model Upper Face Nodes, for Case 2 Analysis

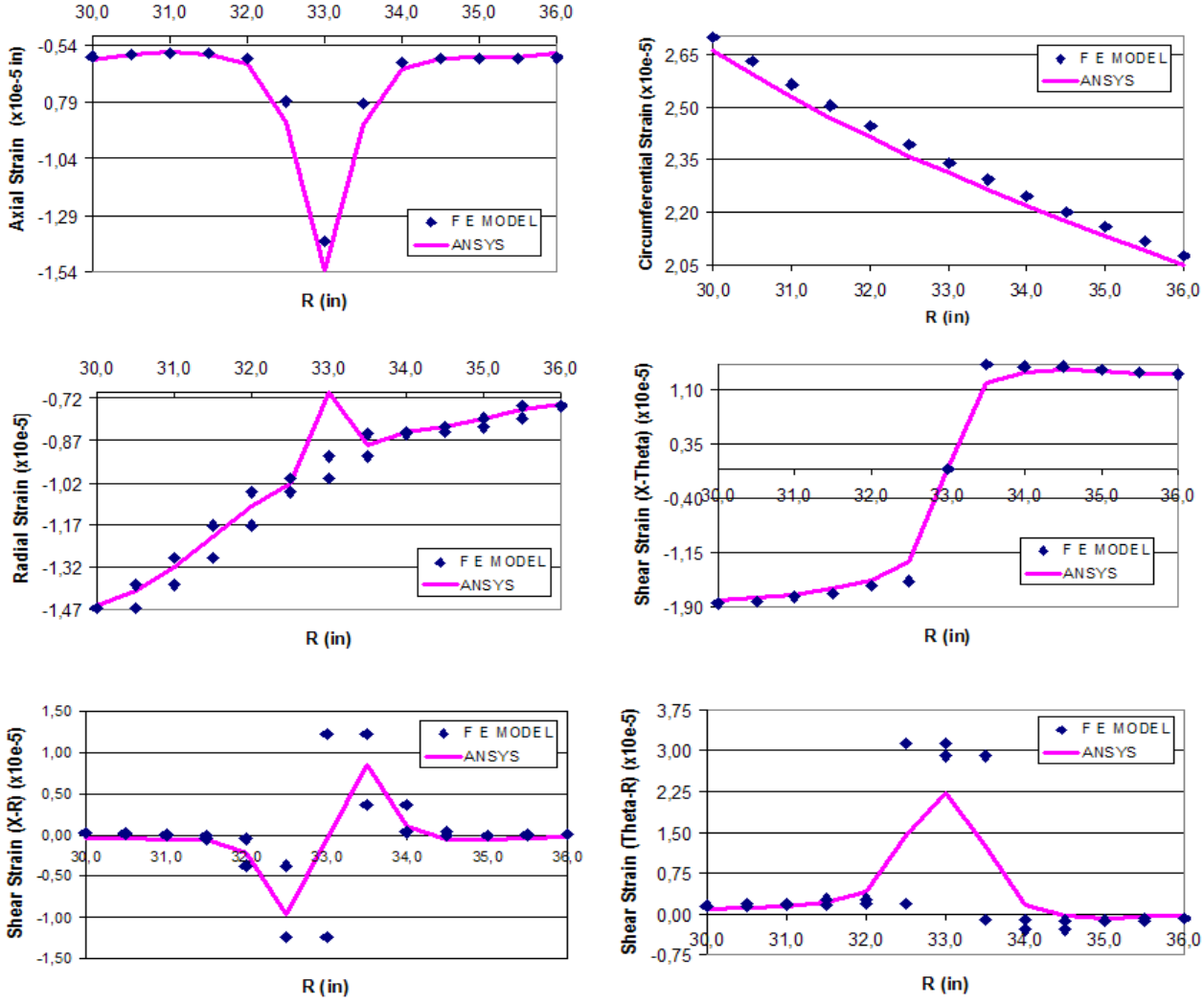

Figure 7 – Strain Components at the Model Upper Face Nodes, for Case 2 Analysis

Figure 7 presents the strain results at the nodes. Major differences between the numerical results are observed at nodes close to the layer-transition node. However, since solutions presented by ANSYS are "smoothed" – a procedure which averages the stress component node values obtained at the two adjoining elements -, it can be concluded that a fairly good agreement in the results is obtained. Comparisons for the stress components in the finite element nodes are shown in Fig. 8. The same path of results, as for the strains, is then observed. Of course, the use of large order elements will improve the solution approximations and provide better solution comparisons.

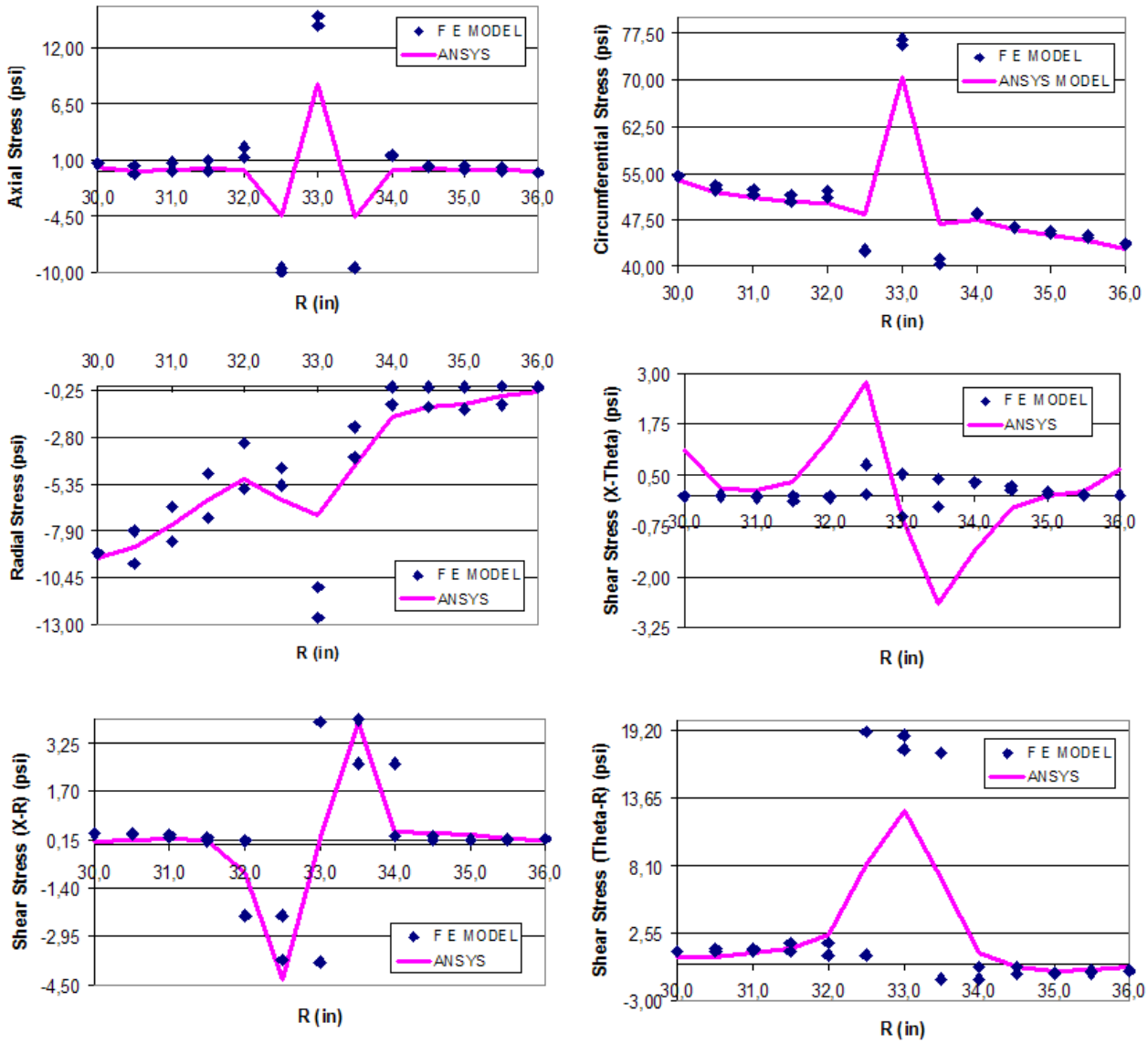

Figure 8 – Stress Components at the Model Upper Face Nodes, for Case 2 Analysis

Conclusions

The formulation of an axisymmetric finite element for composite material modeling, in linear analysis, has been presented and implemented. The solution results of sample analyses have been presented and compared to other analytical and numerical solutions, which indicates the element applicability. It has been shown that the element predicts the significant displacements and, strains and stresses, for the finite element approximation used. However, the total element formulation is based on a number of assumptions and further detailed studies are still required in order to identify the limit of range of problems for which the element can be employed.

ACKNOWLEDGMENTS

The authors gratefully acknowledge the support provided by PUC-Rio for G. P. Guimarães graduate studies.

REFERENCES

Bathe, K. J., 1996, *Finite Element Procedures*, Prentice Hall.

Fung, Y. C., 1965, *Foundations of Solid Mechanics*, Prentice-Hall, Englewood Cliffs, NJ, pp. 114.

Guimarães, G. P., 2006, Uma Formulação de Elementos Finitos Axissimétricos para Análise de Tubos Laminados em Materiais Compósitos, MSc. Thesis, PUC-Rio, 2006 (in portuguese)

Herakovich, C. T., Nagakar,A.P., and O'Brien, D. A., 1979, "Failure Analysis of Composite Laminates with Free Edges", in *Modern Developments in Composite Materials and Structures*, (J.R Vinson,ed.), ASME.

Herakovich, C. T., 1989, "Edge Effects and Delamination Failures", *J. Strain Anal.*, vol. 24, no. 4, pp. 245-252.

Herakovich, C. T., 1998, *Mechanics of Fibrous Composities,* John Wiley & Sons.

Lardner, T. J. and Archer, R. R., 1994, *Mechanics of Solids, an Introduction,* ,McGraw-Hill, Inc..

Lekhnnitskii,S.G., 1950, "Teoriia Uprugosti Anisotropnovo Tela, Government Publishing House for Technical-Theoretical Works", Moscow; transl. *Theory of Elasticity of an Anisotropic Elastic Body,* Holden-Day, Inc., San Francisco, 1963,pp. 243-273.

Pagano, N. J., 1971, "Stress Gradients in Laminated Composite Cylinders", *J. Composite Materials*, vol. 5, pp. 260-265.

Reissner, E., Tsai, W. T., 1974, "Pure Bending, Stretching and Twisting of Anisotropic Cylindrical Shells", *J. Applied. Mechanics*, vol.4, pp. 168-174.

Scherrer, R. E., 1967, "Filament-Wound Cylinders with Axial-Symmetric Loads", *J. Composite Materials*, vol. 1, pp.344-355.

Wilson, J. F., Orgill, G., 1986, "Linear Analysis of Uniformly Stressed, Orthotropic Cylindrical Shells", *J. Applied Mechanics*, vol. 53, pp. 249-256.

RESPONSIBILITY NOTICE

The authors are the only responsible for the printed material included in this paper.